Nonadiabatic selection rules for the photoabsorption of H^- and He

H. R. Sadeghpour*
Joint Institute for Laboratory Astrophysics, Boulder, Colorado 80309-0440
(Received 1 November 1990)

The method of hyperspherical coordinates is used in obtaining very highly excited two-electron adiabatic potential curves up to the $n=12$ hydrogenic threshold. The present numerical effort exploits the analytic nature of the solutions to the Schrödinger equation at small and large distances to diagonalize the hyperspherical Hamiltonian in the combined basis set. Numerical deficiencies resulting from a linear dependency of the total nonorthogonal basis set are overcome in an automatic fashion. A high degree of diabaticity is observed which limits the channel interaction to within a select set of hyperspherical channels. The validity of this quasiconstant of motion as reported by H. R. Sadeghpour and C. H. Greene (SG) [Phys. Rev. Lett. **65**, 313 (1990)] for H^- is investigated for the photoabsorption of He and higher-z members of the He isoelectronic sequence. A generalized two-electron Rydberg formula capable of predicting the positions of the dominant He (ridge and valley) resonances is given. A new feature of the very-highly-excited resonance structure for H^- and He [observed only recently by Domke *et al.*, Phys. Rev. Lett. **66**, 1306 (1991)] is discussed. Semiempirical multichannel-quantum-defect fits are also made to the photodetachment spectra of H^-, supporting the conclusions reached in SG.

I. INTRODUCTION

The study of "two-electron" atoms has remained an active field of research, both in experiment and theory, due to its fundamental importance as the prototype for "many-particle" investigations. Detailed analysis of electron-electron correlation effects in doubly excited states has advanced tremendously since the introduction of high-energy synchrotron photons to atomic spectroscopy in the early 1960s.[1,2] A group-theoretic approach to the systematics of these resonances has uncovered approximate symmetries and correlation quantum numbers that have helped greatly in the classification scheme of the two-electron spectra.[3,4] Numerical "experiments"[5–10] aimed at calculating accurate positions and widths for these autoionizing states have greatly aided our understanding of quantitative aspects of these complexes. A molecular-orbital (MO) description of two-electron states has also shed some light on the general pattern of electron-electron correlation.[11,12]

The method of adiabatic hyperspherical (HS) coordinates was first introduced to the study of electron-correlation effects by Macek[13] in 1968 and has since developed into a powerful tool for understanding these types of processes.[14–16] In this representation, the two electrons are treated equally by introducing a joint coordinate system: a hyperradius R giving a measure of the "size" of the complex and a hyperangle α defining the degree of radial correlation between "valence" electrons. The adiabatic approximation [analogous to the Born-Oppenheimer (BO) approximation for diatomic molecules] has proved remarkably valuable in interpreting the correlation patterns of doubly excited states in the spectrum of He or H^-.[13–16] In this approximation, the two-electron Hamiltonian in HS coordinates is diagonalized parametrically in R as in BO, and the resulting eigenvalues serve as potential-energy channels for electronic motion. Unlike the BO approximation, the adiabatic HS approximation does not rest on any obvious physical justification. The adiabaticity in R derives mainly from the analogy to the BO frozen-nuclei assumption. The remarkable success of the adiabatic approximation in explaining the correlating nature of the multiply excited states and their classification has nonetheless been the major force behind its use.

Sadeghpour and Greene[17] (SG) used this approximation to calculate for the first time the very highly excited $^1P^\circ$ states of H^- up to the $n=12$ hydrogenic threshold. In doing so, Ref. 17 utilized the fact that solutions to the Schrödinger equation are analytically known at small and at large R. The HS Hamiltonian was diagonalized in the combined representative basis set. (This procedure had first been recommended by Lin[18] and was recently employed by Koyama *et al.*[19,20] for the study of high-lying excited states below the $n=7$ hydrogenic threshold.) The problem of linear dependency of eigensolutions obtained from diagonalization in a nonorthogonal basis set was resolved by transforming the adiabatic Hamiltonian into a representation in which the overlap matrix between basis functions is diagonal. A very high degree of diabaticity (weak coupling) between different adiabatic channels was observed and interpreted in terms of contour plots of the two-electron density. It was shown that only those HS channels with similar angular and radial nodal structure have appreciable channel interaction. Those channels whose correlation characteristics influence the photodetachment spectra of H^- were identified and classified with quantum numbers for the bending vibration of the three-body floppy rotor. A generalized two-electron formula was also given which described the positions of most of the observed Feshbach resonances in H^-, to date.

The aim of this article is to give details of the numerical techniques employed for the present calculation, to expand on the major findings of SG and to generalize them for He and its isoelectronic ions, and also to offer a possible explanation for the discrepancy that exists between the observed resonances in H^- and He.[21,22] A two-electron Rydberg-Rydberg formula is derived for helium and analogous to that in SG for H^-, permitting the classification of very highly excited two-electron states of He. This formula assumes a pure Coulomb force which the outer electron feels in the field of an excited He^+ core, and ignores the effect of the dipole field whose presence in H^- is responsible for the formation of quasibound states. The general agreement observed between the experimental data and the level positions predicted with this formula lends support to this assumption and also magnifies the importance of the Coulomb attraction for the doubly excited states of He. The analysis of this paper suggests that it is just this Coulomb force which causes the differences observed in the photoabsorption spectra of H^- and He.

High doubly excited levels calculated in the adiabatic approximation are also compared with the experiments and some available calculations. Semiempirical multichannel quantum-defect theory[16,23,24] (MQDT) fits are also made to the H^- photodetachment spectra in support of the conclusions of SG. A novel feature of these very highly excited states of H^- and He, namely, the perturbation of broad resonances in a hydrogenic manifold by the narrow Rydberg or dipole resonances converging to a lower manifold, very recently observed in He,[25] is discussed.

II. THE HYPERSPHERICAL REPRESENTATION

The method of HS coordinates has been of intense interest in the area of correlated electron motion; see, for instance, the review article by Lin (Ref. 14). In the section the method will be briefly sketched, and the remainder of the section will be devoted to the numerical technique used to obtain the HS potential curves.

In the HS representation the six-dimensional two-electron Hamiltonian is transformed into an equation in $R=(r_1^2+r_2^2)^{1/2}$, $\alpha=\arctan(r_2/r_1)$, and $\Omega\equiv(\alpha,\hat{\mathbf{r}}_1,\hat{\mathbf{r}}_2)$. The full rescaled two-electron Schrödinger equation then reads (in a.u.)

$$\left[\frac{\partial^2}{\partial R^2}-\frac{\Lambda^2-\frac{1}{4}}{R^2}+2\left[E-\frac{C(\alpha,\theta_{12})}{R}\right]\right]\Psi(R;\Omega)=0\ , \tag{1a}$$

where

$$\Lambda^2=-\frac{\partial^2}{\partial\alpha^2}+\frac{l_2^2}{\cos^2\alpha}+\frac{l_2^2}{\sin^2\alpha} \tag{1b}$$

is the squared "grand" angular momentum operator[13] describing collective rotations of the two electrons on the surface of a six-dimensional hypersphere. The quantity

$$C(\alpha,\theta_{12})=-\frac{z}{\cos\alpha}-\frac{z}{\sin\alpha}+\frac{1}{(1-\sin2\alpha\cos\theta_{12})^{1/2}} \tag{1c}$$

acts an an "effective" charge for the system with z the nuclear charge and $\theta_{12}=\arccos(\hat{\mathbf{r}}_1\cdot\hat{\mathbf{r}}_2)$.

It was suggested by Macek[13] that despite the fact that the two operators Λ^2 and C do not commute, the total operator

$$\hat{U}(R;\Omega)=[\Lambda^2/2R^2+C(\alpha,\theta_{12})/R]$$

can nevertheless be diagonalized at each R such that the eigenvalues act as potential-energy curves and the eigenfunctions serve as adiabatic channel functions,

$$\hat{U}(R;\Omega)\Phi_\mu(R;\Omega)=U_\mu(R)\Phi_\mu(R;\Omega)\ . \tag{2}$$

The adiabatic approximation assumes that the off-diagonal coupling matrix elements between the HS channels, $\langle\Phi_\mu|\partial/\partial R\,\Phi_\nu\rangle$ and $\langle\Phi_\mu|\partial^2/\partial R^2\Phi_\nu\rangle$ for $\mu\neq\nu$, are negligible compared to the energy separation between them.

To obtain these potential curves, the fixed R Hamiltonian in Eq. (2) is diagonalized using a linear combination of nonorthogonal basis functions,

$$\Phi_\mu(R;\Omega)=\sum_i\phi_i c_{i\mu}\ . \tag{3}$$

The first part of the basis set in $\{\phi_i\}$ includes eigenfunctions of the grand angular momentum operator of Eq. (1b), i.e.,[15]

$$\Lambda^2 u_{l_1l_2m}(\Omega)=(l_1+l_2+2m+2)^2u_{l_1l_2m}(\Omega)\ , \tag{4a}$$

where

$$u_{l_1l_2m}(\Omega)=N_{l_1l_2m}\left[f_{l_1l_2m}(\alpha)Y_{l_1l_2LM}(\hat{\mathbf{r}}_1,\hat{\mathbf{r}}_2)+(-1)^{l_1+l_2-L+S}f_{l_1l_2m}\left[\frac{\pi}{2}-\alpha\right]\times Y_{l_2l_1LM}(\hat{\mathbf{r}}_1,\hat{\mathbf{r}}_2)\right]\ , \tag{4b}$$

with

$$f_{l_1l_2m}(\alpha)=(\sin\alpha)^{l_2+1}(\cos\alpha)^{l_1+1}\times{}_2F_1(-m,l_1+l_2+m+2;l_2+\tfrac{3}{2};\sin^2\alpha)\ . \tag{4c}$$

Here, $Y_{l_1l_2LM}(\hat{\mathbf{r}}_1,\hat{\mathbf{r}}_2)$ is the well-known coupled spherical harmonic, ${}_2F_1(\ )$ is proportional to a Jacobi polynomial in $\cos2\alpha$, and m is a non-negative integer indexing the nodal structure of the HS harmonics in α. $N_{l_1l_2m}$ is a normalization constant. The augmented two-electron basis functions representing the asymptotic channel functions are constructed from properly symmetrized one-electron orbitals,

$$y_{n_1l_1n_2l_2}(\mathbf{r}_1,\mathbf{r}_2)=\frac{1}{\sqrt{2}}[R_{n_1l_1}(r_1)R_{n_2l_2}(r_2)Y_{l_1l_2LM}(\hat{\mathbf{r}}_1,\hat{\mathbf{r}}_2)+(-1)^{l_1+l_2-L+S}R_{n_2l_2}(r_1)\times R_{n_1l_1}(r_2)Y_{l_2l_1LM}(\hat{\mathbf{r}}_1,\hat{\mathbf{r}}_2)]\ . \tag{5}$$

A generalized eigenvalue equation is obtained after substituting into Eq. (2),

$$\underline{U}\mathbf{c}_\mu = U_\mu(R)\underline{Q}\mathbf{c}_\mu \ , \tag{6}$$

in which $\underline{Q}$ is the full overlap matrix between the basis functions. In the limit of infinite numerical percision, this matrix is positive definite. In practice, however, the overlap matrix is nearly singular. To treat the linear dependence caused by this overcompleteness of the full primitive basis set, the HS Hamiltonian is transformed into the representation which diagonalizes the overlap matrix, amounting to an orthogonalization of the total basis set. The transformed Hamiltonian has the form

$$\tilde{\underline{U}} = \underline{o}^{-1/2}\underline{w}^T\underline{U}\,\underline{w}\,\underline{o}^{-1/2} \ . \tag{7}$$

The matrices $\underline{o}$ and $\underline{w}$ are, respectively, the eigenvalue and the eigenvector matrices obtained from the diagonalization of the full overlap matrix $\underline{Q}$ after discarding all eigenvalues of the overlap $o_\beta \leq \epsilon$, where $\epsilon \simeq 10^{-8}$. The matrices $\underline{o}$ and $\underline{w}$ are therefore nonsquare matrices. The transformed matrix $\tilde{\underline{U}}$ now obeys an ordinary eigenvalue equation,

$$\tilde{\underline{U}}\mathbf{a}_\mu = U_\mu(R)\mathbf{a}_\mu \ , \tag{8}$$

where the primitive eigenvectors are $\mathbf{c}_\mu = \underline{w}\,\underline{o}^{-1/2}\mathbf{a}_\mu$.

III. RESULTS

A. $^1P^\circ$ Potential-energy curves

The adiabatic potential-energy curves for the $^1P^\circ$ symmetry relevant to the single-photon ionization of He and the photodetachment of H^- are shown in Figs. 1(b) and 1(a) up to the $n=12$ hydrogenic threshold, respectively. These curves are shown as R-dependent effective quantum numbers

$$\nu_\mu = [-(2/z^2)U_\mu(R)]^{-1/2}$$

versus $\sqrt{R}$. For the present calculation a primitive basis set comprised of 49 HS harmonics and 123 two-electron orbitals was used. The HS harmonics included quantum numbers $l_1=(0,1,2,\ldots,9)$, $l_2=l_1+1$, and $m=(0,1,2,3,4)$. The two-electron basis functions included all the parity-allowed intrashell states with $n_1=n_2$, the intershell states with $n_2=n_1+1$.

A few of the well-known properties of these potential curves are as follows: The sharp avoided crossing between the "+" (the more attractive curves near the nucleus) and "−" (the more repulsive curves) implies that the potential curves preserve their character through the crossing region leading to sets of coupled *diabatic* curves.[14,15] These approximate quantum numbers , "+" and "−," representing the in-phase and out-of-phase motion of the two electrons, have been used to classify these diabatic curves.[2,14,15] In each n manifold, there exist $n-1$ (n) channels of "+ (−)" character, each of which can be specified in the far field region by the near-exact group-theoretic quantum numbers $T=1$ (0) and

$$K = n-1-T, n-3-T, \ldots, -(n-1-T)$$

appropriate to the $^1P^\circ$ final-state symmetry.[3,4] In the asymptotic region, these adiabatic potential curves develop a dipole tail in the case of H^-, and a combined Coulomb and dipole form in He. This dipole field results from the motion of the outer excited electron in the permanent dipole of the hydrogen atom or helium ion produced by the degenerate mixing of excited angular

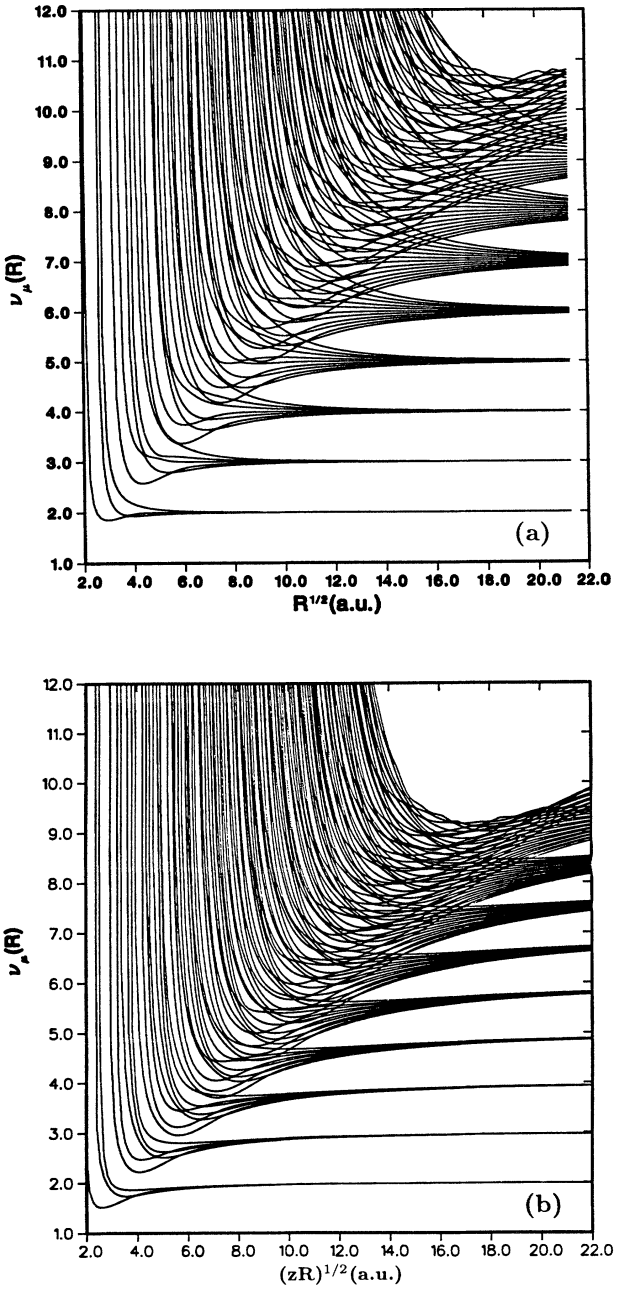

FIG. 1. (a) Adiabatic potential curves for the $^1P^\circ$ symmetry of H^- shown as effective quantum numbers $\nu_\mu(R)$ vs $\sqrt{R}$ (from Ref. 17). (b) Same potential curves for He with the abscissa rescaled with the nuclear charge. Note that in He the attractive Coulomb force binds in all channels. The ridge line is defined as $\nu_W = 18^{-1/4}\sqrt{R}$ for H^- and $\nu_W = (\frac{9}{2})^{-1/4}\sqrt{R}$ for He.

momentum states of H(nl) or $He^+(nl)$. It was pointed out by Gailitis and Damburg[26] that this dipole moment can be obtained using the first-order degenerate perturbation theory. The asymptotic dipole potential in the ${}_n\{v\}^A$-th channel than has the form $a_{{}_n\{v\}^A}/(2R^2)$, where $a_{{}_n\{v\}^A}$ are simply eigenvalues of the Gailitis-Damburg operator.[26,27] The vibrational quantum number ${}_n\{v\}^A$ is defined as ${}_n\{v\}^A=\frac{1}{2}(n-1-K-T)$.[28,17] Approximate expressions for these dipole moments can be written upon using Eq. 38 of Ref. 3. The expressions for the "+" channels with the quantum numbers $K=n-2$, and $K=n-4$ or, alternatively, ${}_n\{v\}^A={}_n\{0\}^+$ and ${}_n\{v\}^A={}_n\{1\}^+$ are

$$
\begin{aligned}
a_{{}_n\{0\}^+} &= -3n^2+\frac{23n}{3}-\frac{2}{3n}-1 , \\
a_{{}_n\{1\}^+} &= -3n^2+\frac{46n}{3}-\frac{8}{3n}-\frac{16}{3} , \\
a_{{}_n\{0\}^+} &= -\frac{3n^2}{2}+\frac{29n}{6}-\frac{1}{3n}-\frac{3}{2} , \\
a_{{}_n\{1\}^+} &= -\frac{3n^2}{2}+\frac{29n}{3}-\frac{4}{3n}-\frac{20}{3} .
\end{aligned}
\tag{9}
$$

The first two expressions belong to H^- while the last two forms are for He. It is worth mentioning here that the existence of the attractive Coulomb force in He is relevant for explaining the different nature of the two-electron resonances observed in He (Refs. 21 and 25) as compared to those in H^-.[22]

B. Generalized two-electron formulas

Two-electron Rydberg formulas,

$$E(n)=-(z-\sigma)^2/(n-\mu)^2 ,$$

have been successful in the classification of the ridge states of H^-, He, and other two-electron atomic systems.[29–31] These formulas derive from an expansion of the two-electron potential, Eq. (1c), about the saddle at $\alpha\simeq\pi/4$ and $\theta_{12}\simeq\pi$. In this section these well-known energy formulas are generalized to predict the positions of all the resonances in a hydrogenic sequence. To this end, the parameters of the generalized formulas are fitted to the adiabatic levels of the ${}_3\{0\}_3^+$, ${}_4\{0\}_4^+$, and ${}_5\{0\}_5^+$ Wannier ridge states in H^- (SG) and He. (No attempts were made to obtain these parameters directly from the first principles.) The optimized values for the screening parameter σ and for the quantum defect μ are 0.1587 and -0.3770 for H^- (as given in SG) and 0.1389 and -0.2043 for He, respectively. Note that the fit was made to only three ridge-riding resonances in order to test the accuracy of the adiabatic calculations and also to gauge the predictive power of these formulas for the higher doubly excited resonances.

For the doubly excited states of He, the two-electron Rydberg formula is combined with the one-electron Rydberg form for the higher resonances into a "Rydberg-Rydberg" formula in a.u.,[17]

$$E(m,n)=\frac{-2}{n^2}\frac{1}{(2m-\mu_n)^2} . \tag{10}$$

In Eq. (10),

$$\mu_n=n-\{-2[2/n^2-(2-\sigma)^2/(n-\mu)^2]\}^{-1/2}$$

is the one-electron quantum defect for the resonances in each ${}_n\{0\}^+$ channel. The Wannier ridge states are classified with $m=n$ and the Rydberg states are described with $m=n+1,n+2,\ldots$ quantum numbers.

The predicted energy levels from Eq. (10), with m treated as continuous, are shown in Fig. 2 along with the experimental results for He.[21] The lowest resonances in each n manifold fall on the Wannier line (unit slope) as expected and the higher Rydberg resonances fall off the ridge line and converge on the nth threshold.

The agreement between the predicted level positions using the two-electron formula for He and the experimental data confirms the Coulombic (Rydberg) nature of these doubly excited states and the small effect of the dipole field on the formation of these quasibound states. It will be seen in Sec. III C that the existence of a handful of resonances lying in the second lowest "+" channel of He with $K=n-4$, or ${}_n\{v\}^A={}_n\{1\}^+$, is a consequence of the presence of this Coulomb field. Similar resonances are absent from the H^- photodetachment spectra observed to date.[17,22]

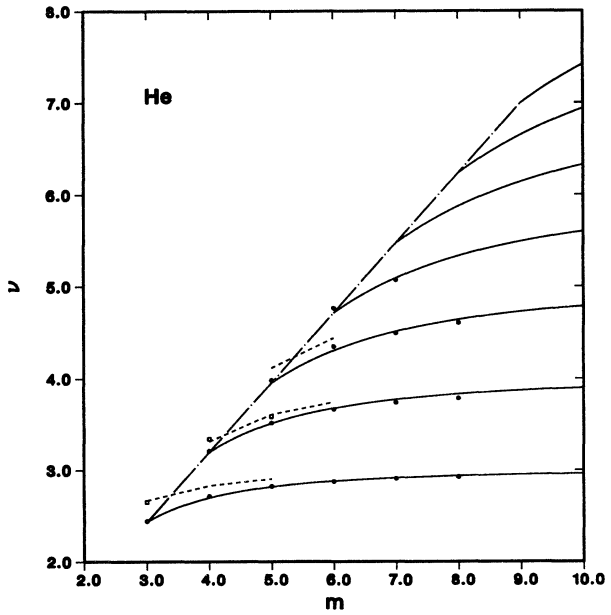

FIG. 2. ${}^1P^\circ$ doubly excited resonances converging on $He^+(n)$ thresholds. The solid lines are from Eq. (10) using the parameters of the ${}_n\{0\}^+$ channels. The experimental resonances of Ref. 21 lying in these channels are given as solid circles. The observed resonances in the second-lowest "+," ${}_n\{1\}^+$, channels are shown as squares. The dashed lines give the positions of these resonances calculated in the adiabatic HS approximation; see also Table II. Note that these same resonances are absent in H^- photodetachment.

C. Physical Interpretation

It was shown in SG that the total dominance of the lowest "+" curves of the hydrogen negative ion, ${}_n\{v\}^A={}_n\{0\}^+$, could be understood in terms of contour plots of the two-electron density as functions of α and θ_{12}. The higher n-manifold "+" channels exhibited extra nodal lines in θ_{12} near the Wannier ridge associated with the degree of bending excitation ${}_n\{v\}^A$. It was consequently argued that only "+" channels with no nodes in θ_{12}, i.e., with zero quantum of bending vibration ${}_n\{v\}^A={}_n\{0\}^+$, similar to those in Fig. 3(a), will be populated. Furthermore, high-lying double excited states would be reached through an initial dipole transition into the lowest channels of Fig. 1 followed by successive nonadiabatic nonradiative transitions between the dominant "+" channels, each having similar radial and angular nodal character in α and θ_{12}.

The above argument holds valid for the helium photoionization process as well. The ${}^1P^\circ$ two-electron density contour plots are shown in Fig. 3 in the $He^+(n=5)$ hydrogenic manifold at $R=25.0$ a.u. near the minima of the adiabatic potential curves where the bulk of the resonant wave functions belonging to these channels are localized. The difference between the photoionization spectra of helium and the photodetachment data of H^- is the observation of a handful of ${}_n\{1\}^+$ resonance lying in the second-lowest "+" channels of He with $K=n-4$. A close look at the Figs. 1(a) and 1(b) provides the clue as to the nature of this discrepancy. In the $He^+(n=3)$ manifold, the ${}_n\{v\}^A={}_3\{1\}^+$ diabatic channel is attractive at all R due to the Coulomb attraction of He^+ and supports resonant states, whereas the ${}_3\{1\}^+$ channel in H^- is totally repulsive due to the repulsive nature of the dipole moment in that channel; see Eq. (9). A calculation of the oscillator strength for the excitation of the resonances belonging to the ${}_3\{0\}^+$ and ${}_3\{1\}^+$ channels in He (in the adiabatic HS approximation) has shown that these resonances receive roughly equal amounts of direct oscillator strength, $\sim 10^{-6}$, from the He ground state.[32] (In H^-, only the ${}_3\{1\}^+$ channel is repulsive.) Inferring from the above arguments, once the ${}_3\{1\}^+$ channel of He is excited by a direct dipole transition (the first time a ${}_n\{1\}^+$ channel appears), the resonances in the higher ${}_n\{1\}^+$ channels are populated by the same nonadiabatic mechanism responsible for the excitation of ${}_n\{0\}_m^+$ resonances in H^- and He while conserving the θ_{12} nodal structure. Generalization of this statement to higher-z isoelectronic members, i.e., Li^+, Be^{2+}, . . . , would imply that the photoexcitation of the doubly excited resonant states in these species will proceed approximately as in He and in each case no more than the first two "+" channels of each hydrogenic manifold will be populated strongly.

These dominant photoexcitation channels are shown in Figs. 4(a) and 4(b) for He and H^-, respectively, In (b) only those diabatic channels with no quanta of bending ${}_n\{v\}^A={}_n\{0\}^+$ are given for H^- (from SG). In (a), the two lowest "+" channels, ${}_n\{0\}^+$ and ${}_n\{1\}^+$, are shown. The level positions are also laid down in each channel. The nonadiabatic ladder line, the loci of the points of closest approach between the curves, is clearly visible as a straight line enroute to the double-ionization continuum limit.

It should be noted that a recent study of the two-electron dynamics in the MO picture has been able to find surprising similarities between the HS and MO representations.[33] The bending quantum number ${}_n\{v\}^A$ is seen to be equal to the number of nodes in one of the

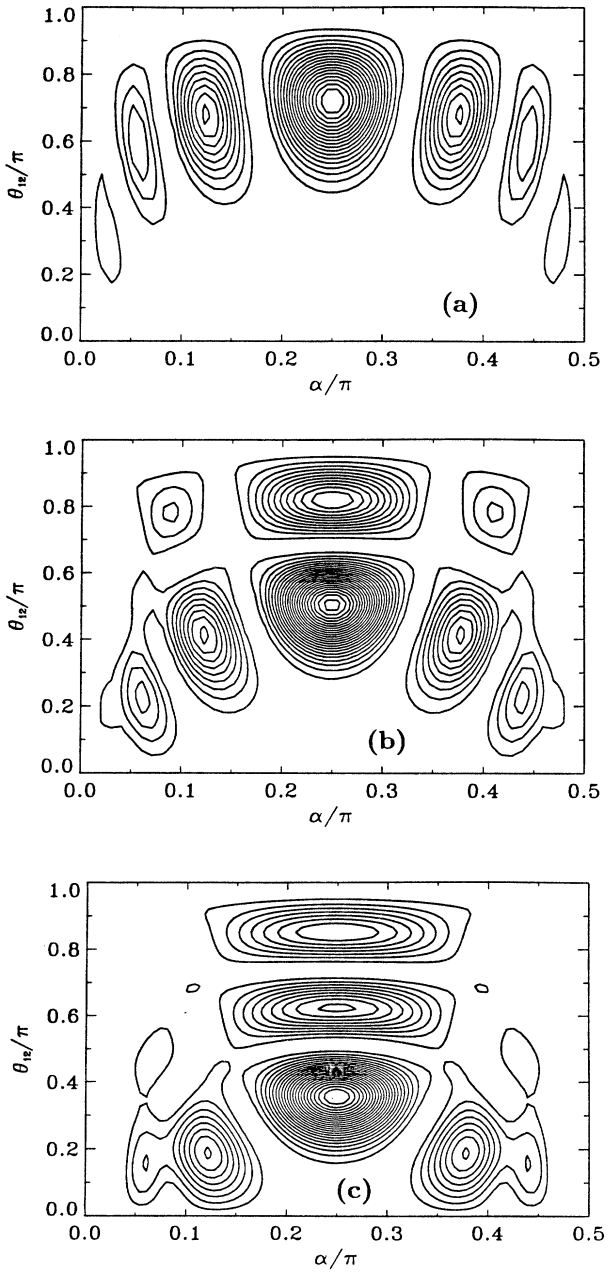

FIG. 3. The adiabatic two-electron density function shown as contour plots vs α and θ_{12}. In (a)–(c), contour plots for the ${}_n\{v\}^A={}_5\{0\}^+$, ${}_5\{1\}^+$, and ${}_5\{2\}^+$ channels of He in the $n=5$ manifold are given at $R=25.0$ a.u., respectively. The v quantum number then respresents the number of the nodal lines in θ_{12}. The radius at which these densities are calculated corresponds to the minima of the respective diabatic channels.

spheroidal directions, the elliptical quantum number n_λ. The number of nodes in α that, using the correlation quantum numbers of this paper, are equal to $2({}_n\{v\}^+ + K)$ is also directly connected with the number of nodal lines in the other spheroidal direction, the hyperbolic quantum number n_μ. Since the nonadiabatic selection rule is described as $\Delta v^+ = 0$ (or $\Delta n_\lambda = 0$ in Ref. 33) and since $|\Delta K| = 1$ from the same considerations that led to the above selection rule, it is readily seen that the preferred change in the number of nodes in α (or n_μ in Ref. 33) for nonradiative transitions is 2 or $\Delta n_\mu = 2$. However, for the ridge-riding two-electron states the nodal structure near $\alpha \simeq \pi/4$ and $\theta_{12} \simeq \pi$ is of outmost importance. Near the potential ridge, the α nodal structures are rather similar (see Fig. 3 of this paper and Ref. 17) and it is the nodal lines of θ_{12} that predominate. It should be stressed that the above selection rule ($\Delta v^+ = 0$ or $\Delta n_\lambda = 0$) describes the preferred direction for nonradiative nonadiabatic transitions, and, as such, is not a statement on the direct photoabsorption process.

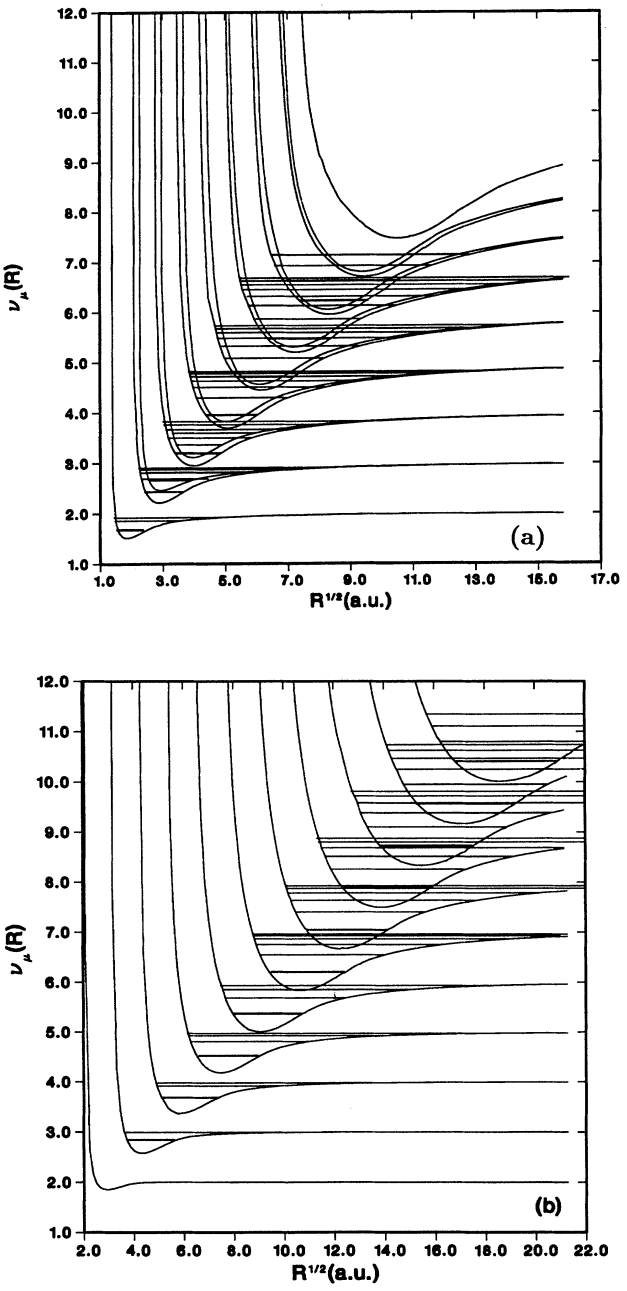

FIG. 4. (a) The diabatic "+" channels with quantum numbers ${}_n\{0\}^+$ and ${}_n\{1\}^+$ within each $He^+(n)$ manifold are plotted as effective quantum numbers vs $\sqrt{R}$. The adiabatic level positions are shown as solid lines in each channel. (b) The ${}_n\{0\}^+$ diabatic channels for H^- (from Ref. 17). The photoabsorption spectra of H^- and He are primarily dominated by these channels. Note also that the region of the avoided crossings is now clearly visible as an imaginary straight line enroute to the double-escape threshold.

One can also speculate that the main autoionizing or autodecay mechanism for these resonances, should be the open continuum of the lowest "+" channel of the next lowest hydrogenic manifold. This speculation follows as a corollary to the postulated nonadiabatic transition process. The implication will be for the nonradiative decay transition ${}_n\{1\}^+ \rightarrow {}_{n-1}\{1\}^+$ for $n > 3$ to occur with roughly the same probability as the transition ${}_n\{0\}^+ \rightarrow {}_{n-1}\{0\}^+$, i.e., ${}_n\{1\}_n^+$ resonances should be approximately as broad as the ${}_n\{0\}_n^+$ states. Calculations of *Ho*[8] corroborate this conjecture. This also explains why the ${}_3\{1\}_3^+$ resonance is so much narrower than the ${}_3\{0\}_3^+$ resonance in He.[8,25,34] Since the first instance a ${}_n\{1\}^+$ channel appears is in the $n = 3$ manifold, the nonradiative decay will be quasiforbidden for the ${}_3\{1\}_3^+$ state.

This decay process can, however, become energetically upset if and when a resonance dips below its first available continuum, as seen for the ridge states, ${}_n\{0\}_n^+$ (the lowest resonant member in a hydrogenic sequence), of high $n \geq 5$ manifolds in Fig. 4. Moreover, this typically broad resonance becomes perturbed by the narrow Rydberg (or dipole) resonances which are converging to the hydrogenic $n-1$ series limit. This feature was pointed out in SG and has been very recently observed in the synchrotron measurements of He.[25]

In H^-, the first instance a ridge state goes below its first available continuum is the ${}_9\{0\}_9^+$ Feshbach resonance. Observation of the perturbation effect on this state is highly difficult since this resonance at $-0.008\,02$ a.u. lies less than 6 meV below $H(n = 8)$ and the dipole resonances converging on this threshold in the range of energy concerned have a width of less than 0.1 meV. The same is true of the ${}_5\{0\}_5^+$ ridge state in He at $-0.127\,99$ a.u. which dips just below $He^+(n = 4)$. The ridge states converging to the higher $He^+(n)$ hydrogenic thresholds, i.e., ${}_6\{0\}_6^+$ and ${}_7\{0\}_7^+$, are on the other hand strongly perturbed by the Rydberg resonances and have indeed been observed with high resolution.[25] The width of these perturbed resonances can no longer be experimentally determined as each resonance is only observed as a global spectral feature. Information about the decay probability of these broad resonances has been extracted with the aid of a three-channel MQDT calculation.[25] It appears that the width of these resonances does not follow the expected scaling with effective quantum number as ν^{-3}.[7-9,21]

D. $^1P^\circ$ Energy Levels

In this section energy levels are calculated in the adiabatic approximation are presented in Tables I and II. The H^- data are calculated by integrating radial solutions in each diabatic channel and matching in the asymptotic region to QDT dipole wave functions.[36] The helium results are obtained, however, by the straightforward integration method. The surprisingly good accord with the observed resonance levels again confirms the smaller interchannel interaction between channels with different radial and angular nodal character.

E. QDT Fits

Drawing from the conclusions of Sec. III C that in each hydrogenic manifold, a single ${}_n\{0\}^+$ channel primarily influences the photodetachment process, the spectrum of H^- is "calculated" assuming a two-channel process for which an analytic form of the resonant cross section exists.[16,36] The weakly closed (energetically inaccessible) channel in which the resonance structure forms is taken to be the ${}_n\{0\}^+$ channel. The open (decay) continuum is assumed to be the ${}_{n-1}\{0\}^+$ channel, although this assumption does not affect the total cross-section fit. The nonresonant background cross section is considered to be a linearly sloping function of energy. The MQDT equations, (see Ref. 16), were fitted to the lowest observed resonance in each n series. The optimized energy-independent parameters (two eigenchannel quantum defects, one mixing angle for the channel interaction, and two dipole matrix elements connecting the final states to the H^- ground state) were then used to predict the rest of the spectra. These fits are shown in Fig. 5, lending support to the conclusions reached in Sec. III C and in SG that a selection rule $\Delta v^+=0$ exists in the photoexcitation of the doubly excited states in H^-. These fits also seem to confirm that the experiment by Harris *et al.* does observe two more dipole resonances not included in the experimental fit.[22] One is the resonant state ${}_5\{0\}_8^+$ in Fig. 5(a), and the other is the excited state ${}_7\{0\}_{10}^+$ in Fig. 5(c). (Table I of Ref. 22 gives a rather large width for the ${}_5\{0\}_7^+$ resonance which can be understood by the presence of the nearby ${}_5\{0\}_8^+$ state not included in the fit.[37]) Minor discrepancies between the fits and the experimental measurements are apparently caused by the total neglect of the energy dependence of the QDT parameters and by the fact that the instrumental resolution of about

TABLE I. Energies of $^1P^\circ$ states of H^-, in a.u., relative to the double-escape threshold. The numbers in parentheses indicate error in the last digits. The calculated values are from the adiabatic hyperspherical treatment.

${}_n\{v\}_m^A$	Calculated	Expt.[1]	Others
${}_n\{0\}_4^+$	−0.036 78		−0.037 16[2] −0.037 35[3] −0.036 735[4]
${}_4\{0\}_5^+$	−0.032 08		−0.032 11[4]
${}_4\{0\}_6^+$	−0.031 44		
${}_5\{0\}_5^+$	−0.024 52	−0.024 518(11)	−0.024 55[2] −0.024 626[3] −0.024 685[4]
${}_5\{0\}_6^+$	−0.021 30	−0.021 393(11)	−0.021 345[4]
${}_5\{0\}_7^+$	−0.020 45	−0.020 617(40)	
${}_6\{0\}_6^+$	−0.017 52	−0.017 333(11)	−0.017 38[2] −0.017 43[3] −0.017 39[4]
${}_6\{0\}_7^+$	−0.015 37	−0.015 249(07)	−0.015 255[4]
${}_6\{0\}_8^+$	−0.014 53	−0.014 594(04)	
${}_6\{0\}_9^+$	−0.014 18	−0.014 333(04)	
${}_7\{0\}_7^+$	−0.012 98	−0.012 877(30)	−0.012 93[5] −0.013 02[3] −0.012 99[4]
${}_7\{0\}_8^+$	−0.011 56	−0.011 289(30)	−0.011 42[6] −0.011 52[4]
${}_7\{0\}_9^+$	−0.010 88	−0.010 914(07)	−0.010 86[6]
${}_7\{0\}_{10}^+$	−0.010 55		
${}_8\{0\}_8^+$	−0.010 09	−0.010 017(40)	−0.009 995[6] −0.010 09[3]
${}_8\{0\}_9^+$	−0.009 05	−0.008 803(07)	
${}_8\{0\}_{10}^+$	−0.008 50	−0.008 660(11)	
${}_8\{0\}_{11}^+$	−0.008 20		
${}_9\{0\}_9^+$	−0.008 02		−0.007 90[6] −0.008 05[3]
${}_9\{0\}_{10}^+$	−0.007 27		
${}_{10}\{0\}_{10}^+$	−0.006 53		
${}_{10}\{0\}_{11}^+$	−0.006 05		
${}_{11}\{0\}_{11}^+$	−0.005 42		
${}_{11}\{0\}_{12}^+$	−0.004 98		
${}_{12}\{0\}_{12}^+$	−0.004 56		
${}_{12}\{0\}_{13}^+$	−0.004 19		

[1]Reference 22.
[2]Reference 7.
[3]Reference 10.
[4]Reference 20.
[5]Reference 9.
[6]Reference 35.

TABLE II. Energies of $^1P^o$ states of He, in a.u., as in Table I.

${}_n\{v\}^A_m$	Calculated	Expt.[1]	Others
${}_4\{0\}^+_4$	−0.195 56	−0.1944(11)	−0.194 54[2] −0.194 871[3] −0.195 55[4]
${}_4\{0\}^+_5$	−0.161 98	−0.1620(11)	−0.161 27[2] −0.161 70[4]
${}_4\{0\}^+_6$	−0.147 85	−0.1489(11)	−0.150 59[2] −0.147 20[4]
${}_4\{0\}^+_7$	−0.140 36	−0.1431(11)	
${}_4\{0\}^+_8$	−0.136 06	−0.1397(11)	
${}_4\{0\}^+_9$	−0.133 35		
${}_4\{0\}^+_{10}$	−0.131 53		
${}_4\{0\}^+_{11}$	−0.130 25		
${}_4\{0\}^+_{12}$	−0.129 31		
${}_4\{0\}^+_{13}$	−0.128 61		
${}_4\{1\}^+_4$	−0.175 76	−0.1794(11)	−0.178 82[2] −0.174 45[4]
${}_4\{1\}^+_5$	−0.153 77	−0.1556(11)	−0.152 75[2] −0.1490[4]
${}_4\{1\}^+_6$	−0.142 87		
${}_4\{1\}^+_7$	−0.137 34		
${}_5\{0\}^+_5$	−0.127 99	−0.1261(11)	−0.126 43[2] −0.126 743[3] −0.127 05[4]
${}_5\{0\}^+_6$	−0.108 21	−0.1057(11)	−0.107 30[2] −0.1080[4]
${}_5\{0\}^+_7$	−0.098 63	−0.0991(11)	
${}_5\{0\}^+_8$	−0.093 04	−0.0943(11)	
${}_5\{0\}^+_9$	−0.089 64		
${}_5\{0\}^+_{10}$	−0.087 41		
${}_5\{0\}^+_{11}$	−0.085 88		
${}_5\{0\}^+_{12}$	−0.084 78		
${}_5\{0\}^+_{13}$	−0.083 96		
${}_5\{1\}^+_5$	−0.118 02		−0.119 18[2] −0.119 05[4]
${}_5\{1\}^+_6$	−0.101 48		
${}_5\{1\}^+_7$	−0.094 19		
${}_6\{0\}^+_6$	−0.089 24	−0.088 1(11)	−0.088 60[2] −0.088 984[3] −0.0888[4]
${}_6\{0\}^+_7$	−0.076 91	−0.0778(11)	−0.78 35[4]
${}_6\{0\}^+_8$	−0.070 12		
${}_6\{0\}^+_9$	−0.066 69		
${}_6\{0\}^+_{10}$	−0.063 98		
${}_6\{0\}^+_{11}$	−0.062 15		
${}_6\{0\}^+_{12}$	−0.060 85		
${}_6\{0\}^+_{13}$	−0.059 90		
${}_6\{1\}^+_6$	−0.083 30		
${}_6\{1\}^+_7$	−0.072 28		
${}_7\{0\}^+_7$	−0.066 12		−0.065 871[3] −0.066 45[4]
${}_7\{0\}^+_8$	−0.058 44		−0.059 30[4]
${}_7\{0\}^+_9$	−0.052 76		
${}_7\{0\}^+_{10}$	−0.049 82		
${}_7\{0\}^+_{11}$	−0.047 79		
${}_7\{0\}^+_{12}$	−0.046 31		
${}_7\{0\}^+_{13}$	−0.045 23		
${}_7\{1\}^+_7$	−0.062 43		
${}_7\{1\}^+_8$	−0.054 83		
${}_8\{0\}^+_8$	−0.051 13		−0.050 714[3]
${}_8\{0\}^+_9$	−0.046 26		
${}_8\{0\}^+_{10}$	−0.042 16		
${}_8\{0\}^+_{11}$	−0.039 53		
${}_8\{0\}^+_{12}$	−0.037 75		
${}_8\{0\}^+_{13}$	−0.036 49		
${}_8\{1\}^+_8$	−0.048 42		
${}_8\{1\}^+_9$	−0.043 06		
${}_8\{1\}^+_{10}$	−0.039 66		
${}_9\{0\}^+_9$	−0.040 40		−0.040 926 76[3]
${}_9\{0\}^+_{10}$	−0.036 45		
${}_9\{0\}^+_{11}$	−0.033 40		
${}_9\{1\}^+_9$	−0.038 88		
${}_9\{1\}^+_{10}$	−0.035 27		

TABLE II. (*Continued*).

${}_n\{v\}^A_m$	Calculated	Expt.[1]	Others
${}_{10}\{0\}^+_{10}$	−0.032 89		−0.032 718[3]
${}_{10}\{0\}^+_{11}$	−0.030 12		
${}_{10}\{0\}^+_{12}$	−0.027 94		

[1]Reference 21.
[2]Reference 8.
[3]Reference 10.
[4]Reference 20.

≃ 8 meV has not been convoluted into the fitted spectrum.

IV. SUMMARY

The objective of this work has been an investigation of the dynamics of very-highly-excited autodetaching two-electron states of H^- and He. In order to be able to carry out the study at such high energies, stable numerical techniques had to be devised to diagonalize the adiabatic HS Hamiltonian. In doing so, accurate $^1P^\circ$ potential-energy curves of H^- and He up to the $n=12$ hydrogenic threshold were obtained.

Significant insights into the photodetachment processes in H^- and in the photoionization of He have been obtained from the study of these adiabatic potential curves. These systematics combined with the very recent experimental observation of these highly excited resonant states of H^- and helium have painted a simple picture of simultaneous excitation and autodecay processes. It is shown that of all the $2n-1$ $^1P^\circ$ channels converging on an nth hydrogenic threshold, only the lowest "+" channel ${}_n\{v\}^A={}_n\{0\}^+$, influences the photospectrum of H^- and, to large extent, He. The small different that exists between the resonances in He and H^- is suggested to be due to the presence of the Coulomb attraction force that binds the outer electron to the ionic He^+ core. Observation of the ${}_n\{1\}^+$ resonances is also predicted in the photospectra of other members of the He isoelectronic sequence.

This general dominance is attributed to the angular characteristics of the channel functions near the minima

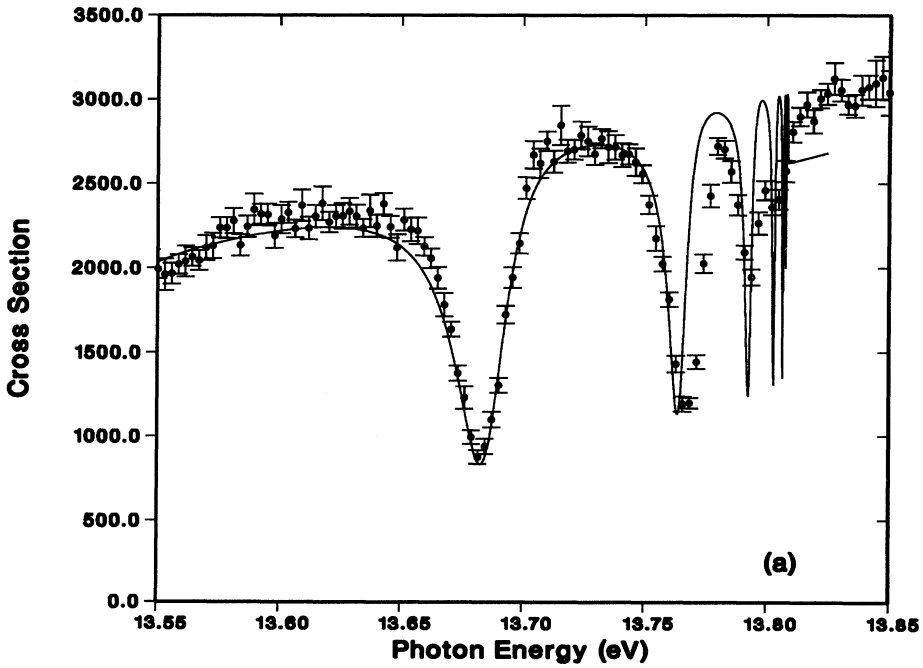

FIG. 5. Two-channel quantum defect (QDT) fits to the photodetachment spectra of H^- in the $n=5-7$ hydrogenic manifolds are shown in (a)–(c), respectively. The experimental data are from Ref. 22. The quantum-defect parameters are assumed to be energy independent. The overall good accord with experiment emphasizes the general dominance of the ${}_n\{v\}^A={}_n\{0\}^+$ photodetachment channels.

of the HS potential curves. High-lying doubly excited states are argued to be populated through successive nonadiabatic nonradiative transitions between the like-character channels that preserve $\Delta v^+=0$. The autoionizing or autodetaching mechanism is also postulated to favor the conservation of the $\Delta v^+=0$ selection rule, i.e., the ${}_n\{1\}_m^+$ two-electron states to decay mostly to ${}_{n-1}\{1\}^+$ continua and the ${}_n\{0\}_m^+$ resonances to decay to ${}_{n-1}\{0\}^+$ open channels.

Generalized two-electron energy formulas account for the resonance positions to a good degree of accuracy, al-

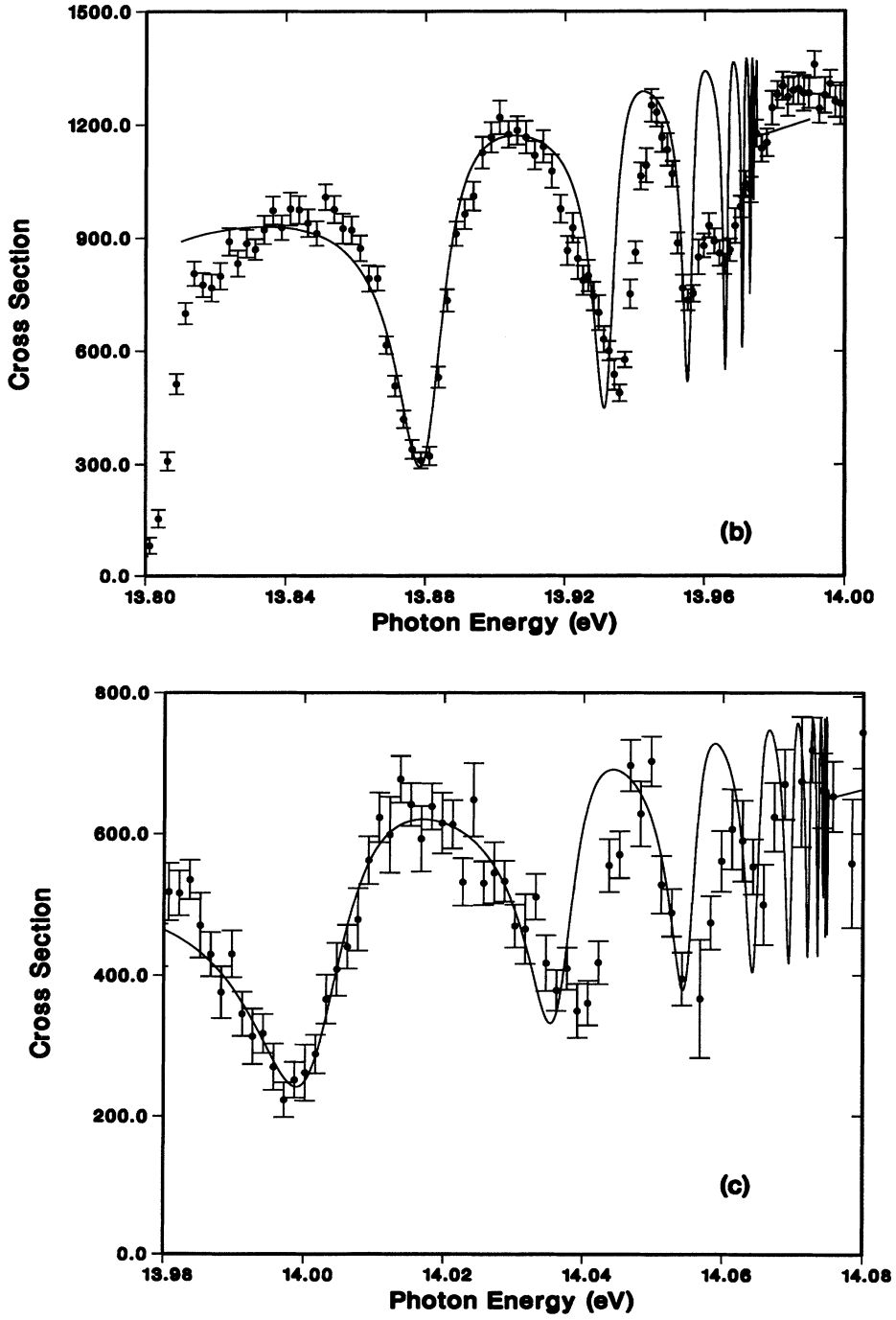

FIG. 5. (*Continued*).

lowing extrapolation to very high quantum numbers. Also, the agreement between the predicted level positions using the two-electron formula for He with the experimental data, (see Fig. 2), is suggestive of the Coulombic nature of these doubly excited states and the diminishing effect of the dipole field on these resonances.

A novel feature of the high-lying two-electron states is discussed in which the broad Feshbach resonances ${}_n\{0\}_n^+$ are perturbed strongly by the narrow dipole or Rydberg resonances forming in the closed $n-1$ channels, i.e., ${}_{n-1}\{0\}^+$. The effects of this interference on the energy positions and line shapes can be explained with the method of MQDT.[25]

ACKNOWLEDGMENTS

I gratefully acknowledge Professor Chris H. Greene for his unconditional support and guidance while I was at Louisiana State University and Joint Institute for Laboratory Astrophysics. I also wish to thank him sincerely for a thoughtful critique of this manuscript. I would also like to thank Dr. M. Cavagnero for many lively discussions, Dr. P. Harris for providing numerical data on the H^- spectra, and Dr. D. Shirley and Dr. G. Kaindl for allowing access to He data prior to publication. The calculations were performed on a Digitial Equipment Corporation DEC station 3100 with financial support from the National Science Foundation.

---

*Present address: Harvard-Smithsonian Center for Astrophysics, 60 Garden Street, Cambridge, MA 02138.

[1]R. P. Madden and K. Codling, Phys. Rev. Lett. **10**, 516 (1963).

[2]J. W. Cooper, U. Fano, and F. Pratts, Phys. Rev. Lett. **10**, 518 (1963).

[3]D. R. Herrick, Phys. Rev. A **12**, 413 (1975).

[4]D. R. Herrick, Adv. Chem. Phys. **52**, 1 (1983).

[5]Y. K. Ho, Phys. Rep. **99**, 1 (1983).

[6]J. Callaway, Phys. Lett. **75A**, 43 (1979); Phys. Rev. A **37**, 3692 (1988).

[7]Y. K. Ho and J. Callaway, Phys. Rev. A **34**, 130 (1986).

[8]Y. K. Ho, J. Phys. B **15**, L691 (1982).

[9]Y. K. Ho, Phys. Rev. A **41**, 1492 (1990).

[10]C. A. Nicolaides and Y. Komninos, Phys. Rev. A **35**, 999 (1987).

[11]J. M. Feagin and J. S. Briggs, Phys. Rev. Lett. **75**, 984 (1986).

[12]J. M. Rost and J. S. Briggs, J. Phys. B **21**, L233 (1988).

[13]J. H. Macek, J. Phys. B **1**, 831 (1968).

[14]C. D. Lin, Adv. At. Mol. Phys. **22**, 77 (1986), and references therein.

[15]C. D. Lin, Phys. Rev. A **10**, 1986 (1974); Phys. Rev. Lett. **35**, 1150 (1975).

[16]C. H. Greene, J. Phys. B **13**, L31 (1980).

[17]H. R. Sadeghpour and C. H. Greene, Phys. Rev. Lett. **65**, 313 (1990).

[18]C. D. Lin, Phys. Rev. A **23**, 1585 (1981).

[19]N. Koyama, H. Fukuda, T. Motoyama, and M. Matsuzawa, J. Phys. B **19**, L331 (1986).

[20]N. Koyama, A. Takafuji, and M. Matsuzawa, J. Phys. B **22**, 533 (1989).

[21]M. Zubek, G. C. King, P. M. Rutter, and F. H. Read, J. Phys. B **22**, 3411 (1989).

[22]P. G. Harris, H. C. Bryant, A. H. Mohagheghi, R. H. Reeder, H. Sharifian, C. Y. Tang, H. Tootoonchi, J. B. Donahue, C. R. Quick, D. C. Rislove, W. W. Smith, and J. E. Stewart, Phys. Rev. Lett. **65**, 309 (1990).

[23]U. Fano and A. R. P. Rau, *Atomic Collisions and Spectra* (Academic, Orlando, 1986).

[24]C. H. Greene, Phys. Rev. A **23**, 149 (1980).

[25]M. Domke, C. Xue, A. Puschmann, T. Mandel, E. Hudson, D. A. Shirley, G. Kaindl, C. H. Greene, H. R. Sadeghpour, and H. Peterson, Phys. Rev. Lett. **66**, 1306 (1991).

[26]M. Gailitis and R. Damburg, Proc. Phys. Soc. London **82**, 192 (1963).

[27]H. R. Sadeghpour and C. H. Greene, Phys. Rev. A **39**, 115 (1989).

[28]S. Watanabe and C. D. Lin, Phys. Rev. A **34**, 823 (1986).

[29]F. H. Read, J. Phys. B **10**, 449 (1977).

[30]A. R. P. Rau, J. Phys. B **16**, L699 (1983).

[31]Q. Molina, Phys. Rev. A **39**, 3298 (1989); C. A. Nicolaides, M. Chrysos, and Y. Komninos, J. Phys. B **21**, L73 (1988); L. Kim and C. H. Greene, Phys. Rev. A **38**, 2361 (1988).

[32]H. R. Sadeghpour, Ph.D. thesis, Louisiana State University, 1990.

[33]J. M. Rost, J. S. Briggs, and J. M. Feagin, Phys. Rev. Lett. **66**, 1642 (1991).

[34]J. M. Rost and J. S. Briggs, J. Phys. B **23**, L339 (1990).

[35]Y. K. Ho (private communication).

[36]C. Greene, U. Fano, and G. Strinati, Phys. Rev. A **19**, 1485 (1979).

[37]P. G. Harris, Ph.D. thesis, University of New Mexico, 1990.